

# Thermodynamics of the $\text{Al}_2\text{O}_3\text{--Al}_4\text{C}_3$ system

## I. Thermochemical functions of Al oxide, carbide and oxycarbides between 298 and 2100 K

J.-M. Lihrmann\*

LIMHP, UPR CNRS 1311, Avenue J.-B. Clément, 93430 Villetaneuse, France

Received 27 March 2006; received in revised form 24 June 2006; accepted 30 June 2006

Available online 8 November 2007

### Abstract

A consistent set of thermochemical functions are proposed for aluminium oxide ( $\text{Al}_2\text{O}_3$ ), carbide ( $\text{Al}_4\text{C}_3$ ) and oxycarbides ( $\text{Al}_4\text{O}_4\text{C}$ ,  $\text{Al}_2\text{OC}$ ), including Gibbs free energies, enthalpies and entropies of formation as well as heat capacities, between 298 and 2100 K. Heat capacities of the base components of the Al–O–C system are also given. All equations are compared with existing functions in terms of relative errors, pointing important discrepancies for aluminium carbide and aluminium oxycarbide  $\text{Al}_2\text{OC}$ . When some are used to determine equilibrium partial pressures of carbon monoxide in classical high temperature solid–gas reactions, these discrepancies are confirmed or amplified. As a consequence, the present equations are suggested to describe the thermodynamic behaviour of aluminium carbide and aluminium oxycarbide  $\text{Al}_2\text{OC}$ .

© 2007 Published by Elsevier Ltd.

**Keywords:** Chemical properties;  $\text{Al}_2\text{O}_3$ ; Carbides; Aluminium oxycarbides; Refractories;  $\text{Al}_4\text{C}_3$ ; Thermodynamic data

### 1. Introduction

Aluminium carbide ( $\text{Al}_4\text{C}_3$ ) is a quite interesting material, although its high reactivity with water precludes its use in many instances. It forms readily when previously and sufficiently mixed and milled elemental powders of aluminium and graphite are heated in Argon above some hundreds of degrees.<sup>1</sup> It has also been observed to form at room temperature, as 2–4 nm grain size precipitates, by implantation of carbon ions into pure aluminium, though at a carbon concentration below the stoichiometric value.<sup>2</sup> Whereas  $\text{Al}_4\text{C}_3$  is currently being used as a surrogate for beryllium carbide in the tokamak dust particle removal studies,<sup>3</sup> it is also a soft reactant for  $\text{Al}_2\text{O}_3$ , able to form two Al oxycarbides which act as very efficient binding agents in 95+ %  $\text{Al}_2\text{O}_3$  refractory bricks, with higher thermal resistance, mechanical strength and abrasive properties than the classical graphite, mullite and sialon binders.<sup>4,5</sup> Furthermore, the thermodynamic properties of  $\text{Al}_4\text{C}_3$  are very important in the case of Al/SiC metal matrix composites since they inform on the possible formation of this compound at Al/SiC inter-

faces, where it is indeed frequently observed, without omitting to mention the high catalytic ability of  $\text{Al}_4\text{C}_3$  particles to nucleate  $\alpha\text{-Al}$  phase in hypoeutectic Al–Si alloys.<sup>6</sup> While on the other hand aluminium oxide offers a multitude of industrial applications as a major ceramic material,<sup>7</sup> the present paper is aimed at updating the various thermochemical functions of the solid compounds within the  $\text{Al}_2\text{O}_3\text{--Al}_4\text{C}_3$  system. In this purpose, a set of equations are at first proposed and compared with previously suggested equations, then the improvements are shown by investigating their implications on some high temperature reactions often encountered in the carbothermal reduction of alumina.

### 2. Rationale

The stable phase-equilibrium diagram of the  $\text{Al}_2\text{O}_3\text{--Al}_4\text{C}_3$  system is presented in its usual form in Fig. 1. It features both oxycarbides as intermediate compounds,<sup>8</sup> the richer in  $\text{Al}_2\text{O}_3$  decomposing peritectically at 2163 K while the equimolar compound is stable between a eutectoid plateau slightly above 1983 K and a peritectic plateau near 2260 K; this diagram also includes a eutectic reaction about 2123 K. The solubilities of all four compounds, which are not represented in Fig. 1, are dis-

\* Tel.: +33 1 49 40 34 23; fax: +33 1 49 40 34 14.  
E-mail address: [lihmann@limhp.univ-paris13.fr](mailto:lihmann@limhp.univ-paris13.fr).

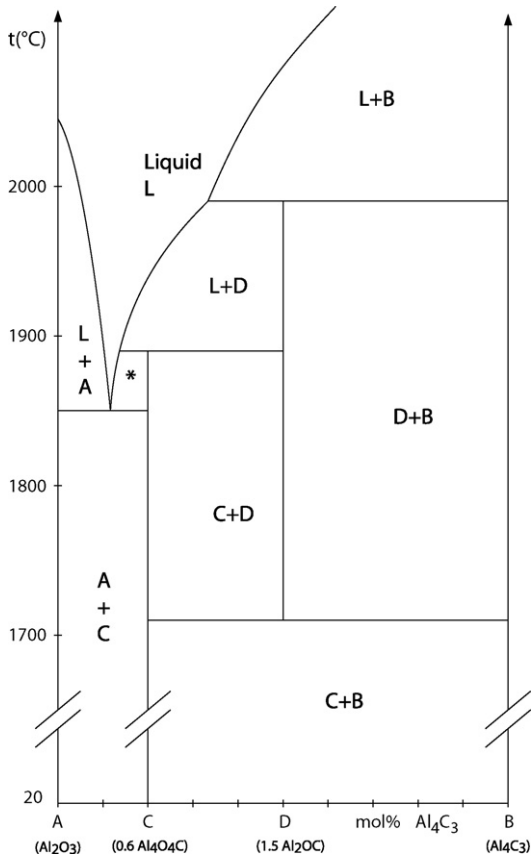


Fig. 1. Phase diagram of the  $\text{Al}_2\text{O}_3$ – $\text{Al}_4\text{C}_3$  system (\* = L + C).

cussed in Part 2 of this work and are shown to be negligibly small. As it is often the case in ceramic systems,<sup>9</sup> there exists in addition a metastable  $\text{Al}_2\text{O}_3$ – $\text{Al}_4\text{C}_3$  diagram,<sup>8,10,11</sup> which is observed for higher cooling rates and not referred to in the present study.

A previous paper<sup>12</sup> listed the Gibbs free energies of formation of these compounds between 1000 and 2100 K. In a first step, these functions were extended to the melting temperature of aluminium (933 K), and the enthalpies and entropies of formation of solid compounds were obtained, as well as their heat capacities, once those of the base components  $\text{C}_{(s)}$ ,  $\text{Al}_{(l)}$  and  $\text{O}_{2(g)}$  were defined between 933 and 2100 K. In a second step, heat capacities of both solid compounds and base components were defined between 298 and 933 K, what permitted to determine enthalpies, entropies and Gibbs free energies of formation of all solid compounds in this interval; the molar heat of fusion of aluminium was taken as 10,500 J.

Aluminium oxycarbides are not widely used so far, nor are the thermodynamic properties of aluminium carbide often discussed or in question, so that the references available for comparison are altogether rather scarce.<sup>13–17</sup>

### 3. Results

All equations suggested in this section concern standard properties (normal pressure), in SI units (J, mole, K), of solids in their field of thermodynamic stability, whence the narrow temperature range for  $\text{Al}_2\text{OC}$ : 1983.05–2100 K; usually, three

Table 1  
Standard Gibbs free energies of formation of solid compounds in the C–Al–O system, in SI units (J, mole, K)

$\text{Al}_2\text{O}_3$	$298 \leq T \leq 933$	(1)
	$\Delta_f G^\circ = -1692098.49628 + 469436.372462 \times 10^{-3} T - 20.79 T \ln T - 1087.525 \times 10^{-6} T^2 + 2911.2095 \times 10^{-9} T^3 + 1506.970625 \times 10^3 / T$	
	$933 \leq T \leq 1500$	(2)
	$\Delta_f G^\circ = -1703587.779 + 362016.573 \times 10^{-3} T - 2320.216 \times 10^{-3} T \ln T - 5438.306 \times 10^{-6} T^2 + 258.189 \times 10^{-9} T^3 + 1331.985 \times 10^3 / T$	
	$1500 \leq T \leq 2100$	(3)
	$\Delta_f G^\circ = -1750864.909 + 660614.800 \times 10^{-3} T - 42120.216 \times 10^{-3} T \ln T + 8878.444 \times 10^{-6} T^2 - 649.745 \times 10^{-9} T^3 + 11577.935 \times 10^3 / T$	
$\text{Al}_4\text{C}_3$	$298 \leq T \leq 933$	(4)
	$\Delta_f G^\circ = -198954.518109 - 78152.2033574 \times 10^{-3} T + 19.20 T \ln T - 26031.6 \times 10^{-6} T^2 + 9815.3473333 \times 10^{-9} T^3 - 5908.882 \times 10^3 / T + 792.9 \times 10^6 / T^2 - 36 \times 10^9 / T^3$	
	$933 \leq T \leq 2100$	(5)
	$\Delta_f G^\circ = -209944.693 - 282185.012 \times 10^{-3} T + 51158.268 \times 10^{-3} T \ln T - 15316.705 \times 10^{-6} T^2 + 0.3633 \times 10^{-9} T^3 - 9551.482 \times 10^3 / T + 792.9 \times 10^6 / T^2 - 36 \times 10^9 / T^3$	
$\text{Al}_4\text{O}_4\text{C}$	$298 \leq T \leq 933$	(6)
	$\Delta_f G^\circ = -2334566.14257 + 612528.342841 \times 10^{-3} T - 22.98 T \ln T - 10800.5 \times 10^{-6} T^2 + 7730.60066667 \times 10^{-9} T^3 - 44.5975 \times 10^3 / T + 264.3 \times 10^6 / T^2 - 12 \times 10^9 / T^3$	
	$933 \leq T \leq 1500$	(7)
	$\Delta_f G^\circ = -2352531.936 + 388627.099 \times 10^{-3} T + 13959.135 \times 10^{-3} T \ln T - 12356.643 \times 10^{-6} T^2 + 344.37 \times 10^{-9} T^3 - 1407.847333 \times 10^3 / T + 264.3 \times 10^6 / T^2 - 12 \times 10^9 / T^3$	
	$1500 \leq T \leq 2100$	(8)
	$\Delta_f G^\circ = -2415568.109 + 786758.068 \times 10^{-3} T - 39107.532 \times 10^{-3} T \ln T + 6732.357 \times 10^{-6} T^2 - 866.2056 \times 10^{-9} T^3 + 22253.41934 \times 10^3 / T + 264.3 \times 10^6 / T^2 - 12 \times 10^9 / T^3$	
$\text{Al}_2\text{OC}$	$1983.05 \leq T \leq 2100$	(9)
	$\Delta_f G^\circ = -667653.2006 + 300380.064 \times 10^{-3} T - 19187.316 \times 10^{-3} T \ln T - 2146.087 \times 10^{-6} T^2 - 216.4606 \times 10^{-9} T^3 + 675.484334 \times 10^3 / T + 264.3 \times 10^6 / T^2 - 12 \times 10^9 / T^3$	

Table 2

Standard heat capacities of the base components in the system C–Al–O, in SI units (J, mole, K)

C (graphite)

$$298 \leq T \leq 2100$$

$$C_p^\circ = 24.3 + 0.9446 \times 10^{-3} T - 5.1252 \times 10^6 / T^2 + 1.5858 \times 10^9 / T^3 - 0.144 \times 10^{12} / T^4 \quad (28)$$

Al

$$298 \leq T \leq 933$$

$$C_p^\circ = 29.095 - 9.57485 \times 10^{-3} T + 15.872946 \times 10^{-6} T^2 - 0.268741 \times 10^6 / T^2 \quad (29)$$

$$933 \leq T \leq 2100$$

$$C_p^\circ = 31.750 \quad (30)$$

O<sub>2</sub>

$$298 \leq T \leq 933$$

$$C_p^\circ = 21.42 + 22.6769 \times 10^{-3} T - 9.519090 \times 10^{-6} T^2 + 0.1804845 \times 10^6 / T^2 \quad (31)$$

$$933 \leq T \leq 1500$$

$$C_p^\circ = 34.47 + 1.8412 \times 10^{-3} T - 1.455811 \times 10^6 / T^2 \quad (32)$$

$$1500 \leq T \leq 2100$$

$$C_p^\circ = 34.717 + 1.730 \times 10^{-3} T - 1.6352695 \times 10^6 / T^2 \quad (33)$$

Table 3

Standard heat capacities of the solid compounds in the system C–Al–O, in SI units (J, mole, K)

Al<sub>2</sub>O<sub>3</sub>

$$298 \leq T \leq 933$$

$$C_p^\circ = 111.11 + 17.0407 \times 10^{-3} T - 3.2806965 \times 10^6 / T^2 \quad (34)$$

$$933 \leq T \leq 1500$$

$$C_p^\circ = 117.525216 + 13.638412 \times 10^{-3} T - 1.549134 \times 10^{-6} T^2 - 4.8476865 \times 10^6 / T^2 \quad (35)$$

$$1500 \leq T \leq 2100$$

$$C_p^\circ = 157.695716 - 15.161888 \times 10^{-3} T + 3.89847 \times 10^{-6} T^2 - 25.60877425 \times 10^6 / T^2 \quad (36)$$

Al<sub>4</sub>C<sub>3</sub>

$$298 \leq T \leq 933$$

$$C_p^\circ = 170.08 + 16.5976 \times 10^{-3} T + 4.5997 \times 10^{-6} T^2 - 4.6328 \times 10^6 / T^2 \quad (37)$$

$$933 \leq T \leq 2100$$

$$C_p^\circ = 148.741732 + 33.46721 \times 10^{-3} T - 2.1798 \times 10^{-9} T^2 + 3.727364 \times 10^6 / T^2 \quad (38)$$

Al<sub>4</sub>O<sub>4</sub>C

$$298 \leq T \leq 933$$

$$C_p^\circ = 206.50 + 29.60 \times 10^{-3} T - 1.93 \times 10^{-6} T^2 - 5.75009 \times 10^6 / T^2 \quad (39)$$

$$933 \leq T \leq 1500$$

$$C_p^\circ = 206.280865 + 29.340286 \times 10^{-3} T - 2.06622 \times 10^{-6} T^2 - 5.221127334 \times 10^6 / T^2 \quad (40)$$

$$1500 \leq T \leq 2100$$

$$C_p^\circ = 259.841532 - 9.060114 \times 10^{-3} T + 5.1972336 \times 10^{-6} T^2 - 32.90257768 \times 10^6 / T^2 \quad (41)$$

Al<sub>2</sub>OC

$$1983.05 \leq T \leq 2100$$

$$C_p^\circ = 124.345816 + 6.101774 \times 10^{-3} T + 1.2987636 \times 10^{-6} T^2 - 7.293803418 \times 10^6 / T^2 \quad (42)$$

temperature intervals are distinguished: 298–933, 933–1500 and 1500–2100 K.

Gibbs free energies of formation of solid compounds are listed in Table 1; the corresponding enthalpies and entropies of formation, readily derived from the former, are listed in Tables A.1 and A.2 (see Appendix A).

Heat capacities of base components are listed in Table 2; those of solid compounds are in Table 3 and illustrated in Fig. 2. Eqs. (35), (36), (38), (40), (41) and (42) were obtained using appropriate functions of Table A.1 as well as Eqs. (28), (30), (32) and (33); below 933 K, Eqs. (28), (29), (31), (34), (37) and (39) were necessary to determine the low temperature functions of Tables A.1, A.2 and 1. Eq. (28) is suggested<sup>18</sup> by SGTE and Eq. (30) is in close agreement with numerous references. Eq. (32) through (34), which obey the most classical form for a heat

capacity function,<sup>19</sup> were obtained from Janaf<sup>15</sup> data, in addition with Refs. 13 and 14 for Eq. (34). The remaining equations include an additional quadratic term; they were obtained using data from Janaf<sup>15</sup> for (29), (31) and (37), and from Ref. 13 for (37) and (39).

#### 4. Discussion

Eq. (1) through (9) establish that Al<sub>4</sub>O<sub>4</sub>C oxycarbide is a more stable compound than Al<sub>2</sub>O<sub>3</sub>, itself more stable than Al<sub>2</sub>OC and finally Al<sub>4</sub>C<sub>3</sub>; on a unit constituent basis, 1/5 Al<sub>2</sub>O<sub>3</sub> is more stable than 1/9 Al<sub>4</sub>O<sub>4</sub>C, itself more stable than 1/4 Al<sub>2</sub>OC and finally 1/7 Al<sub>4</sub>C<sub>3</sub> (see Part 2).

Among all equations of Tables 1, A.1 and A.2, those which are closely approximated by linear functions are compared

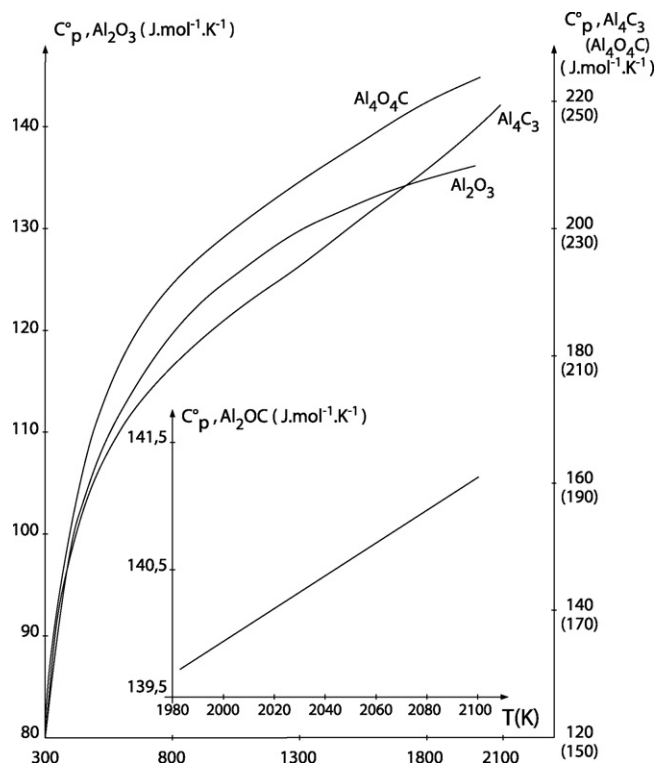


Fig. 2. Calculated heat capacities ( $\text{J mol}^{-1} \text{K}^{-1}$ ) of solid compounds  $\text{Al}_2\text{O}_3$ ,  $\text{Al}_4\text{C}_3$ ,  $\text{Al}_4\text{O}_4\text{C}$  and  $\text{Al}_2\text{OC}$  between 300 and 2100 K.

with their linear counterparts in Table A.3. It appears that 9 among the 10 functions describing Gibbs free energies of formation are perfectly linear, thereby verifying, over fairly extended temperature intervals, Ülich approximation of nearly temperature-independent enthalpies and entropies of reactions; this approximation is more thoroughly studied in Appendix A (Table A.4). The last  $\Delta_f G^\circ$  function may be said to be close to linear with a high accuracy, and so are the various  $\Delta_f S^\circ$  equations listed in the table; this statement becomes somewhat less true for

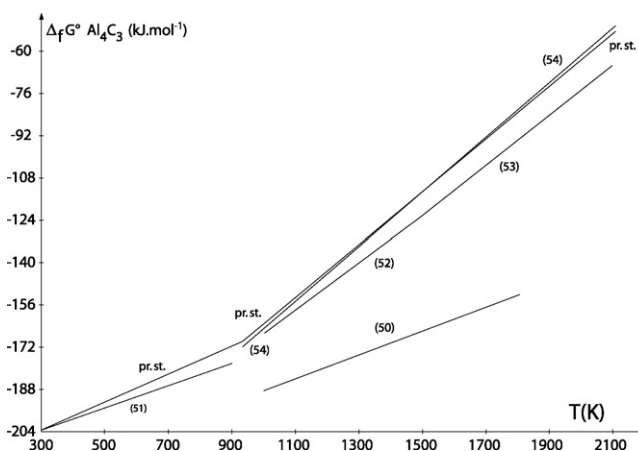


Fig. 3. Gibbs free energies of formation of aluminium carbide.

the standard enthalpies of formation. It can also be seen that the relative errors between each function and its linear approximation are extremely small at all temperatures, most of them smaller than  $\pm 2.5 \times 10^{-2}\%$  and never exceeding either  $-0.1295\%$  or  $+0.2582\%$ .

Other existing equations for Gibbs free energies, enthalpies and entropies of formation of the solid compounds in the C–Al–O system, as mentioned in Refs. 14 through 17, are listed in Tables 4 and 5. Eq. (56) through (59) were derived from Eqs. (43) and (44), and all functions numbered with a superscript are linear estimates of discrete data from Ref. 15. Table A.5 shows that the relative errors between estimates and data do not exceed  $\pm 0.321\%$ .

These other existing functions are compared with those of Tables 1, A.1 and A.2 in Table 6 (here all Janaf data used for comparison are the actual values, rather than the modelled ones; the same also applies for Table 9). It clearly appears that the situation with aluminium carbide is very different from that of aluminium oxide and aluminium oxycarbide  $\text{Al}_4\text{O}_4\text{C}$ . With

Table 4

Other existing functions for Gibbs free energies of formation of solid compounds in the C–Al–O system, in SI units (J, mole, K)

			References
$\text{Al}_2\text{O}_3$			
$298 \leq T \leq 933$ ,	$\Delta_f G = -1676989.04 + 366.68576 T - 16.65232 T \log T$	(43)	14
$933 \leq T \leq 1800$ ,	$\Delta_f G = -1697699.84 + 385.8485 T - 15.69 T \log T$	(44)	14
$298 \leq T \leq 900$ ,	$\Delta_f G^\circ = -1674978.0303 + 313.0035 T$	(45) <sup>a</sup>	15
$1000 \leq T \leq 1500$ ,	$\Delta_f G^\circ = -1688989.7482 + 328.1463 T$	(46) <sup>a</sup>	15
$1500 \leq T \leq 2100$ ,	$\Delta_f G^\circ = -1678617.5043 + 321.2909 T$	(47) <sup>a</sup>	15
$933 \leq T \leq 1800$ ,	$\Delta_f G^\circ = -1676000 + 320 T$	(48)	16
$933 \leq T \leq 2100$ ,	$\Delta_f G = -1677123 + 321.72 T$	(49)	17
$\text{Al}_4\text{C}_3$			
$1000 \leq T \leq 1800$ ,	$\Delta_f G = -233048.80 + 45.1872 T$	(50)	14
$298 \leq T \leq 900$ ,	$\Delta_f G^\circ = -216261.9943 + 42.8561 T$	(51) <sup>a</sup>	15
$1000 \leq T \leq 1500$ ,	$\Delta_f G^\circ = -263934.8888 + 94.1962 T$	(52) <sup>a</sup>	15
$1500 \leq T \leq 2100$ ,	$\Delta_f G^\circ = -265655.0109 + 95.3578 T$	(53) <sup>a</sup>	15
$933 \leq T \leq 2100$ ,	$\Delta_f G = -268000 + 103.6 T$	(54)	17
$\text{Al}_4\text{O}_4\text{C}$			
$933 \leq T \leq 2100$ ,	$\Delta_f G = -2333307 + 463.214 T$	(55)	17

<sup>a</sup> From discrete values (see Table A.5).

Table 5

Other existing functions for enthalpies and entropies of formation of solid compounds in the Al–C–O system, in SI units (J, mole, K)

				References
<b>Al<sub>2</sub>O<sub>3</sub></b>				
298 ≤ T ≤ 933,	Δ <sub>f</sub> H = −1676989.04 + 7.232 T	(56)		14
298 ≤ T ≤ 933,	Δ <sub>f</sub> S = −359.45375 + 7.232 ln T	(57)		14
933 ≤ T ≤ 1800,	Δ <sub>f</sub> H = −1697699.84 + 6.81408 T	(58)		14
933 ≤ T ≤ 1800,	Δ <sub>f</sub> S = −379.03442 + 6.81408 ln T	(59)		14
1000 ≤ T ≤ 1500,	Δ <sub>f</sub> H° = −1708924.5158 + 16.2303 T	(60) <sup>a</sup>		15
1500 ≤ T ≤ 2100,	Δ <sub>f</sub> H° = −1716624.6697 + 21.3533 T	(61) <sup>a</sup>		15
<b>Al<sub>4</sub>C<sub>3</sub></b>				
1000 ≤ T ≤ 1500,	Δ <sub>f</sub> H° = −258362.797 − 4.4757 T	(62) <sup>a</sup>		15
1500 ≤ T ≤ 2100,	Δ <sub>f</sub> H° = −262521.4937 − 1.7304 T	(63) <sup>a</sup>		15

<sup>a</sup> From discrete values (see Table A.5).

Table 6

Comparison of Gibbs free energies, enthalpies and entropies of formation of solid compounds in the C–Al–O system

Equations compared	Intervals of relative errors (%)	
Janaf–(1); Janaf–(2); Janaf–(10)	Abs. R.E. < 0.1	[−0.0371; −0.0302]; [−0.0285; +0.0411]; [−0.0313; −0.0640]
(43)–(1); (48)–(3); (49)–(3); (56)–(10); (58)–(11); (58)–(12)	Abs. R.E. < 0.2	[−0.1563; −0.1965]; [−0.0411; +0.1242]; [−0.1632; −0.0047]; [−0.0605; −0.1803]; [−0.1721; −0.0213]; [−0.0213; +0.1224]
(44)–(2); Janaf–(3); Janaf–(11)	Abs. R.E. < 0.3	[−0.1845; −0.2359]; [+0.0411; +0.2637]; [+0.0686; −0.2042]
(44)–(3); (55)–(8)	Abs. R.E. < 0.4	[−0.2359; −0.3230]; [−0.3321; −0.2568]
(48)–(2); (49)–(2); Janaf–(12); (59)–(20)	Abs. R.E. < 0.5	[−0.4564; −0.0411]; [−0.4915; −0.1632]; [−0.2042; −0.4133]; [−0.1170; +0.4974]
(55)–(7); (59)–(21)	Abs. R.E. < 1	[−0.6022; −0.3321]; [+0.4974; +0.9468]
Janaf–(4); (54)–(5); Janaf–(13); Janaf–(14); (57)–(19)	Abs. R.E. < 4.5	[−0.2994; +3.4758]; [+1.0598; −4.3307]; [−2.5552; −0.3318]; [+0.0396; +2.8664]; [+1.5368; −0.1031]
(50)–(5); Janaf–(5)	Abs. R.E. > 4.5	[+13.3129; +45.7238]; [+4.0182; +19.5089]

Al<sub>2</sub>O<sub>3</sub>, all Gibbs free energies and enthalpies of formation are in agreement within 0.5% absolute relative error, and this abs. relative error does not exceed 1.54% for the entropy of formation. With Al<sub>4</sub>O<sub>4</sub>C only one reference is available for comparison, but the abs. relative error in free energies of formation is smaller

than 1%. In contrast, the various equations suggested as Gibbs free energies of formation of Al<sub>4</sub>C<sub>3</sub> are presented in Fig. 3. While there is a fair agreement between Eq. (54) and this study in the entire temperature interval 933–2100 K, although the relative error exceeds −4.33% at 2100 K, the discrepancy with

Table 7

Room temperature values of thermochemical functions for the solid compounds in the C–Al–O system, in SI units

	Δ <sub>f</sub> G°	Δ <sub>f</sub> H°	Δ <sub>f</sub> S°	S°	References
Al <sub>2</sub> O <sub>3</sub>	Not mentioned	Not mentioned	Not mentioned	50.95	13
	−1579995	−1673600 ± 6275	−318.25	51.05 ± 0.40	14
	−1581878.35	−1675273.6	−313.4069	50.936	15
	m.d.	−1674000	m.d.	50.60	16
	−1582464.93132	−1675846.68502	−313.361589598	50.830460402	Present
Al <sub>4</sub> C <sub>3</sub>	−118830 ± 33470	−150200 ± 33470	−105.2685	101.90	13
	m.d.	−195393 ± 41850	m.d.	131 ± 10.5	14
	−203350.768	−215685.2	−41.3907	88.97	15
	−203959.516247	−221196.315368	−57.8416077886	72.5026922114	Present
Al <sub>4</sub> O <sub>4</sub> C	−2140953 ± 33470	−2272330 ± 33470	−440.8631	101.90	13
	−2189428.06056	−2320352.60684	−439.344115035	89.693384965	Present
Al <sub>2</sub> OC	−664837.6 ± 41840	−717137.6 ± 41840	−175.5034	27.196	13
		Unstable below 1983.05 K			8,10–12, Present

Table 8

Other existing functions for the heat capacities of base components and solid compounds in the C–Al–O system, in SI units (J, mole, K)

			References
C (graphite)			
298 ≤ T ≤ 2100	$C_p = 17.155 + 4.2677 \times 10^{-3} T - 0.87864 \times 10^6 / T^2$	(64)	14
	$C_p = 17.2 + 4.27 \times 10^{-3} T - 0.879 \times 10^6 / T^2$	(65)	16
Al (solid)			
298 ≤ T ≤ 933	$C_p = 20.67 + 12.3846 \times 10^{-3} T$	(66)	14
	$C_p = 20.7 + 12.4 \times 10^{-3} T$	(67)	16
O <sub>2</sub> (g)			
298 ≤ T ≤ 2100	$C_p = 29.96 + 4.184 \times 10^{-3} T - 0.16736 \times 10^6 / T^2$	(68)	14
	$C_p = 30 + 4.18 \times 10^{-3} T - 1.7 \times 10^5 / T^2$	(69)	16
Al <sub>2</sub> O <sub>3</sub>			
298 ≤ T ≤ 2100	$C_p = 115.02 + 11.7989 \times 10^{-3} T - 3.506192 \times 10^6 / T^2$	(70)	13
298 ≤ T ≤ 1800	$C_p = 114.56 + 12.8867 \times 10^{-3} T - 3.430880 \times 10^6 / T^2$	(71)	14
298 ≤ T ≤ 900	$C_p = 103.76 + 26.4429 \times 10^{-3} T - 2.903696 \times 10^6 / T^2$	(72) <sup>a</sup>	15
1000 ≤ T ≤ 1500	$C_p = 113.11 + 12.9905 \times 10^{-3} T - 1.242119 \times 10^6 / T^2$	(73) <sup>a</sup>	15
1500 ≤ T ≤ 2100	$C_p = 127.32 + 6.6605 \times 10^{-3} T - 10.947147 \times 10^6 / T^2$	(74) <sup>a</sup>	15
298 ≤ T ≤ 1800	$C_p = 106.6 + 17.8 \times 10^{-3} T - 2.85 \times 10^6 / T^2$	(75)	16
Al <sub>4</sub> C <sub>3</sub>			
298 ≤ T ≤ 2100	$C_p = 185.35 + 13.3470 \times 10^{-3} T - 5.183976 \times 10^6 / T^2$	(76)	13
298 ≤ T ≤ 600	$C_p = 100.75 + 132.2144 \times 10^{-3} T$	(77)	14
298 ≤ T ≤ 900	$C_p = 154.3 + 30.36 \times 10^{-3} T - 4.3146 \times 10^6 / T^2$	(78) <sup>a</sup>	15
1000 ≤ T ≤ 1500	$C_p = 179.20 + 6.8332 \times 10^{-3} T - 9.833936 \times 10^6 / T^2$	(79) <sup>a</sup>	15
1500 ≤ T ≤ 2100	$C_p = 189.20 + 2.4711 \times 10^{-3} T - 17.333857 \times 10^6 / T^2$	(80) <sup>a</sup>	15
Al <sub>4</sub> O <sub>4</sub> C			
298 ≤ T ≤ 2100	$C_p = 215.14 + 20.1669 \times 10^{-3} T - 6.401520 \times 10^6 / T^2$	(81)	13
Al <sub>2</sub> OC			
298 ≤ T ≤ 2100	$C_p = 100.12 + 8.3680 \times 10^{-3} T - 2.895328 \times 10^6 / T^2$	(82)	13

<sup>a</sup> From discrete values (see Table A.5).

functions 51 through 53, soon appears following an almost perfect agreement at room temperature, and keeps increasing as the temperature increases. As to Eq. (50), it is clearly far remote towards too negative values.

The same trends appear in Table 7 which gives the room temperature values, at 298 K, of the thermochemical functions discussed so far, as well as the entropy values of solid compounds. Ref. 13, which was the first and most ancient to include

Table 9

Comparison of heat capacities of base components and solid compounds in the Al–C–O system

Equations compared	Intervals of relative errors (%)	
Janaf–(31); Janaf–(32); Janaf–(33)	Abs. R.E. < 0.1	[−0.0466; +0.0508]; [+0.0643; −0.0683]; [−0.0818; +0.0743]
(81)–(40); (81)–(41)	Abs. R.E. < 0.5	[+0.3279; −0.3202]; [−0.3649; −0.0919]
(71)–(34); (71)–(35); Janaf–(35); (81)–(39)	Abs. R.E. < 1.0	[+0.8688; −0.4878]; [−0.6104; +0.0168]; [+0.2150; −0.6533]; [−0.8958; +0.9187]
Janaf–(29); (70)–(34); (70)–(35); (70)–(36); (71)–(36); Janaf–(34); Janaf–(36)	Abs. R.E. < 1.5	[−1.3949; +1.4339]; [+0.4314; −1.0161]; [−1.2381; −0.9019]; [−0.9017; +1.2673]; [+0.0169; +1.1454]; [−1.2984; +0.6300]; [−0.0339; +1.2601]
(68)–(31); (69)–(31); (69)–(32); (69)–(33); (75)–(36)	Abs. R.E. < 2.5	[+1.6087; −2.4566]; [+1.6786; −2.3556]; [−2.4885; −1.0785]; [−1.0796; +1.9625]; [−0.2345; +1.9084]
Janaf–(28); (66)–(29); (67)–(29); (68)–(32); (68)–(33); (75)–(34); (75)–(35); (76)–(38)	Abs. R.E. < 5.0	[+1.1006; −2.5860]; [−0.7724; −4.4853]; [−0.6318; −4.3416]; [−2.5890; −1.1703]; [−1.1714; +2.6330]; [+0.7095; −2.7761]; [−2.8341; −0.2345]; [+3.9619; −3.6075]
(64)–(28); (65)–(28); (76)–(37); (77)–(37); Janaf–(37)	Abs. R.E. < 15.0	[+12.0672; −5.0801]; [−4.8495; +12.3711]; [+6.1857; +3.9615]; [+12.0445; +2.8780]; [−7.2147; −5.5130]
Janaf–(38); (82)–(42)	Abs. R.E. > 15.0	[−5.5591; −15.3317]; [−20.4471; −20.6747]

Table 10  
Carbon monoxide partial pressures (atm) at equilibrium in some carbothermal reactions

Reaction	$p_{\text{CO}}$ experimental (Ref. 13)	$p_{\text{CO}}$ calculated (present study)
$2\text{Al}_2\text{O}_3 + 3\text{C} = \text{Al}_4\text{O}_4\text{C} + 2\text{CO}_{(\text{g})}$ (a)	$2.24 \times 10^{-2}$ (1820 K) $\rightarrow$ 0.4803 (2100 K)	$0.7347 \times 10^{-2}$ (1820 K) $\rightarrow$ 0.238125 (2100 K)
$\text{Al}_2\text{O}_3 + 3\text{C} = \text{Al}_2\text{OC} + 2\text{CO}_{(\text{g})}$ (b)	$4.21 \times 10^{-2}$ (1720 K) $\rightarrow$ 0.5263 (2030 K)	$4.8714 \times 10^{-2}$ (1983.05 K) $\rightarrow$ 0.087448 (2030 K)
$\text{Al}_4\text{O}_4\text{C} + 6\text{C} = \text{Al}_4\text{C}_3 + 4\text{CO}_{(\text{g})}$ (c)	$3.29 \times 10^{-2}$ (1920 K) $\rightarrow$ 0.4079 (2100 K)	$1.6973 \times 10^{-2}$ (1920 K) $\rightarrow$ 0.147823 (2100 K)
$\text{Al}_4\text{O}_4\text{C} + \text{Al}_4\text{C}_3 = 8\text{Al}_{(\text{l})} + 4\text{CO}_{(\text{g})}$ (d)	$1.10 \times 10^{-2}$ (1920 K) $\rightarrow$ 0.2524 (2200 K)	$0.1868 \times 10^{-2}$ (1920 K) $\rightarrow$ $3.2882 \times 10^{-2}$ (2100 K) (0.132105 <sub>5</sub> at 2200 K)

Table 11  
Measured high temperature Al equilibrium vapour pressure, vs. Al equilibrium saturated vapour pressure

Temperature (K)	$P$ (mmHg)	
	Measured <sup>13</sup>	Sat. vapour pressure <sup>20</sup>
1902	13	2
2000	45	5
2080	125	10
2167	299	20

thermodynamic data on the  $\text{Al}_2\text{O}_3$ – $\text{Al}_4\text{C}_3$  system, is extremely misleading on  $\text{Al}_4\text{C}_3$ , especially for  $\Delta_f G^\circ$  and  $\Delta_f S^\circ$  and to a minor extent  $\Delta_f H^\circ$ ; as to the room temperature entropy value of this compound, both Refs. 13 and 14 are problematic. In order to determine  $S^\circ$  knowing  $\Delta_f S^\circ$ , the following well accepted base component values were used ( $\text{J mol}^{-1} \text{K}^{-1}$ ):  $S_{298}^\circ(\text{C}_{(\text{s})}) = 5.6861$ ;  $S_{298}^\circ(\text{Al}_{(\text{s})}) = 28.3215$ ;  $S_{298}^\circ(\text{O}_{2(\text{g})}) = 205.0327$ .

Some other existing functions for heat capacities of base components and solid compounds in the Al–C–O system, are listed in Table 8 and compared with equations of this study, in Table 9. Here again, those with abs. relative errors larger than 10% pertain to aluminium carbide (Refs. 14 and 15) and aluminium oxycarbide  $\text{Al}_2\text{OC}$  (Ref. 13) as well as, more surprisingly, to graphite (Refs. 14 and 16). In all other cases, it can be seen that there is a reasonable agreement.

At this point it is timely to address the high temperature affinity of the solids discussed so far, for graphite, and to investigate the equilibrium pressure of some reactions at various temperatures between 1500 and 2100 K. For this purpose the linear expressions of Table A.3 are used, as well as  $\Delta_f G^\circ(\text{CO}_{(\text{g})}) = -117172.0234 - 84.4077 T$ , within less than 0.5% abs. relative error with Refs. 14–16. Table 10 mentions four of such reactions, labelled (a) through (d), and reports measured<sup>13</sup> equilibrium vapour pressures of carbon monoxide. In the same table, comparison with values calculated from the present study shows that the measured values are unquestionably higher. That they are in fact much too high is best seen when one compares (Table 11) the equilibrium vapour pressure of liquid aluminium as reported in Ref. 13, with the Al saturated vapour pressure as determined from Ref. 20. It then becomes clear that the measured vapour pressures are erroneous, as well as the heats and free energies of formation for  $\text{Al}_2\text{OC}$ ,  $\text{Al}_4\text{O}_4\text{C}$  and  $\text{Al}_4\text{C}_3$  reported in Ref. 13, since these were all calculated from pressure measurements.

## 5. Conclusion

A consistent set of thermochemical functions, including Gibbs free energies of formation, enthalpies and entropies of reactions, and heat capacities, are proposed for the base components and solid compounds in the C–Al–O system. The paper points out important discrepancies existing for aluminium carbide and aluminium oxycarbide  $\text{Al}_2\text{OC}$ , and suggests new equations to define these compounds more properly.

## Acknowledgements

Numerous previous or present colleagues are acknowledged for their interest in aluminium oxycarbides, including: Pr. M. Daire, B. Willer and T. Zambetakis, Dep. of Materials Science, Ecole de chimie, Strasbourg (France); J.L. Huang and R.A. Cutler, Ceramtec Com-pany, Salt Lake City (USA); D. Broussaud, Rhone Poulenc Research Center, Aubervilliers, and Pr. F. Thévenot, Ecole des mines, Saint-Etienne (France); C. Qiu and Pr. R. Metselaar, University of Technology, Eindhoven (Netherlands); J. Tirlocq, P. Descamps and F. Cambier, Industr. Ceramic Research Center, Mons (Belgium); M. Bougoin, Céramiques et Composites, Bazet (France); Pr. B. Le Neindre and Pr. A. Vignes, CNRS-LIMHP, Villetaneuse (France); V.E. Grass, Institute of Chemistry, Syktyvkar (Russia).

## Appendix A

The standard enthalpies and entropies of formation of Al oxide, carbide and oxycarbides, as obtained from Table 1 using Gibbs–Helmholtz equation, are listed in Tables A.1 and A.2 below. Table A.3 shows that Gibbs free energies of formation of  $\text{Al}_2\text{O}_3$ ,  $\text{Al}_4\text{C}_3$ ,  $\text{Al}_4\text{O}_4\text{C}$  and  $\text{Al}_2\text{OC}$  vary with temperature essentially like linear functions, confirming Ülich approximation of nearly temperature-independent enthalpies (the constant terms of linear estimates) and entropies (minus the temperature coefficients of linear estimates) of reaction. It is of course an approximation, as shown by the variations of these quantities with temperature, also themselves almost perfectly linear in the various temperature ranges. Table A.4, which compares the ‘constant’ values of  $\Delta_f H^\circ$  and  $\Delta_f S^\circ$  with the actual values of Tables A.1 and A.2, gives the exactness of Ülich approximation.

Discrete data from Ref. 15 could, in most cases, be modelled according to classical functions, and Table A.5 shows that the relative errors with actual values are small.

Table A.1

Standard enthalpies of formation of solid compounds in the C–Al–O system, in SI units (J, mole, K)

Al <sub>2</sub> O <sub>3</sub>	
298 ≤ T ≤ 933	$\Delta_f H^\circ = -1692098.49628 + 20.79 T + 1087.525 \times 10^{-6} T^2 - 5822.419 \times 10^{-9} T^3 + 3013.94125 \times 10^3/T$ (10)
933 ≤ T ≤ 1500	$\Delta_f H^\circ = -1703587.779 + 2320.216 \times 10^{-3} T + 5438.306 \times 10^{-6} T^2 - 516.378 \times 10^{-9} T^3 + 2663.970 \times 10^3/T$ (11)
1500 ≤ T ≤ 2100	$\Delta_f H^\circ = -1750864.909 + 42120.216 \times 10^{-3} T - 8878.444 \times 10^{-6} T^2 + 1299.49 \times 10^{-9} T^3 + 23155.87 \times 10^3/T$ (12)
Al <sub>4</sub> C <sub>3</sub>	
298 ≤ T ≤ 933	$\Delta_f H^\circ = -198954.518109 - 19.20 T + 26031.6 \times 10^{-6} T^2 - (58892.084/3) \times 10^{-9} T^3 - 11817.764 \times 10^3/T + 2378.7 \times 10^6/T^2 - 144 \times 10^9/T^3$ (13)
933 ≤ T ≤ 2100	$\Delta_f H^\circ = -209944.693 - 51158.268 \times 10^{-3} T + 15316.705 \times 10^{-6} T^2 - 0.7266 \times 10^{-9} T^3 - 19102.964 \times 10^3/T + 2378.7 \times 10^6/T^2 - 144 \times 10^9/T^3$ (14)
Al <sub>4</sub> O <sub>4</sub> C	
298 ≤ T ≤ 933	$\Delta_f H^\circ = -2334566.14257 + 22.98 T + 10800.5 \times 10^{-6} T^2 - (46383.604/3) \times 10^{-9} T^3 - 89.195 \times 10^3/T + 792.9 \times 10^6/T^2 - 48 \times 10^9/T^3$ (15)
933 ≤ T ≤ 1500	$\Delta_f H^\circ = -2352531.936 - 13959.135 \times 10^{-3} T + 12356.643 \times 10^{-6} T^2 - 688.74 \times 10^{-9} T^3 - 2815.694666 \times 10^3/T + 792.9 \times 10^6/T^2 - 48 \times 10^9/T^3$ (16)
1500 ≤ T ≤ 2100	$\Delta_f G^\circ = -2415568.109 + 39107.532 \times 10^{-3} T - 6732.357 \times 10^{-6} T^2 + 1732.4112 \times 10^{-9} T^3 + 24506.83868 \times 10^3/T + 792.9 \times 10^6/T^2 - 48 \times 10^9/T^3$ (17)
Al <sub>2</sub> OC	
1983.05 ≤ T ≤ 2100	$\Delta_f H^\circ = -667653.2006 + 19187.316 \times 10^{-3} T + 2146.087 \times 10^{-6} T^2 + 432.9212 \times 10^{-9} T^3 + 1350.968668 \times 10^3/T + 792.9 \times 10^6/T^2 - 48 \times 10^9/T^3$ (18)

Table A.2

Standard entropies of formation of solid compounds in the C–Al–O system, in SI units (J, mole, K)

Al <sub>2</sub> O <sub>3</sub>	
298 ≤ T ≤ 933	$\Delta_f S^\circ = -448.646372462 + 20.79 \ln T + 2.17505 \times 10^{-3} T - 8.7336285 \times 10^{-6} T^2 + 1.506970625 \times 10^6/T^2$ (19)
933 ≤ T ≤ 1500	$\Delta_f S^\circ = -359.696357 + 2.320216 \ln T + 10.876612 \times 10^{-3} T - 0.774567 \times 10^{-6} T^2 + 1.331985 \times 10^6/T^2$ (20)
1500 ≤ T ≤ 2100	$\Delta_f S^\circ = -618.494584 + 42.120216 \ln T - 17.756888 \times 10^{-3} T + 1.949235 \times 10^{-6} T^2 + 11.577935 \times 10^6/T^2$ (21)
Al <sub>4</sub> C <sub>3</sub>	
298 ≤ T ≤ 933	$\Delta_f S^\circ = 58.9522033574 - 19.20 \ln T + 52.0632 \times 10^{-3} T - 29.446042 \times 10^{-6} T^2 - 5.908882 \times 10^6/T^2 + 1.5858 \times 10^9/T^3 - 0.108 \times 10^{12}/T^4$ (22)
933 ≤ T ≤ 2100	$\Delta_f S^\circ = 231.026744 - 51.158268 \ln T + 30.633410 \times 10^{-3} T - 1.0899 \times 10^{-9} T^2 - 9.551482 \times 10^6/T^2 + 1.5858 \times 10^9/T^3 - 0.108 \times 10^{12}/T^4$ (23)
Al <sub>4</sub> O <sub>4</sub> C	
298 ≤ T ≤ 933	$\Delta_f S^\circ = -589.548342841 + 22.98 \ln T + 21.601 \times 10^{-3} T - 23.191802 \times 10^{-6} T^2 - 0.0445975 \times 10^6/T^2 + 0.5286 \times 10^9/T^3 - 0.036 \times 10^{12}/T^4$ (24)
933 ≤ T ≤ 1500	$\Delta_f S^\circ = -402.586234 - 13.959135 \ln T + 24.713286 \times 10^{-3} T - 1.03311 \times 10^{-6} T^2 - 1.407847333 \times 10^6/T^2 + 0.5286 \times 10^9/T^3 - 0.036 \times 10^{12}/T^4$ (25)
1500 ≤ T ≤ 2100	$\Delta_f S^\circ = -747.650536 + 39.107532 \ln T - 13.464714 \times 10^{-3} T + 2.5986168 \times 10^{-6} T^2 + 12.25341934 \times 10^6/T^2 + 0.5286 \times 10^9/T^3 - 0.036 \times 10^{12}/T^4$ (26)
Al <sub>2</sub> OC	
1983.05 ≤ T ≤ 2100	$\Delta_f S^\circ = -281.192748 + 19.187316 \ln T + 4.292174 \times 10^{-3} T + 0.6493818 \times 10^{-6} T^2 + 0.675484334 \times 10^6/T^2 + 0.5286 \times 10^9/T^3 - 0.036 \times 10^{12}/T^4$ (27)



Table A.3

Linear expressions of standard thermochemical functions of Tables 1, A.1 and A.2, in SI units (J, mole, K)

		Reliability coefficient	Interval of relative error ( $10^{-2}\%$ )	
$\text{Al}_2\text{O}_3$	$298 \leq T \leq 933$	$\Delta_f G^\circ = -1675594.0832 + 313.1813T$	1.0000	[−1.37; +2.39]
	$933 \leq T \leq 1500$	$\Delta_f G^\circ = -1691664.2525 + 330.2555T$	1.0000	[−1.36; +1.76]
		$\Delta_f H^\circ = -1705024.4343 + 11.3094T$	0.9974	[+1.13; −1.32]
		$\Delta_f S^\circ = -341.5392 + 0.0093T$	1.0000	[−1.09; +0.33]
	$1500 \leq T \leq 2100$	$\Delta_f G^\circ = -1683596.3293 + 324.8824T$	1.0000	[−1.58; +2.14]
		$\Delta_f H^\circ = -1711318.0314 + 15.5746T$	0.9997	[−0.70; +0.53]
$\Delta_f S^\circ = -340.5310 + 0.0087T$		0.9997	[−0.52; +2.94]	
$\text{Al}_4\text{C}_3$	$298 \leq T \leq 933$	$\Delta_f G^\circ = -219728.7859 + 53.8955T$	0.9999	[+14.3; −10.63]
	$933 \leq T \leq 1500$	$\Delta_f G^\circ = -263439.3224 + 100.5843T$	1.0000	[+ 3.88; −4.53]
	$1500 \leq T \leq 2100$	$\Delta_f G^\circ = -262173.9443 + 99.8502T$	1.0000	[−12.95; +25.82]
$\text{Al}_4\text{O}_4\text{C}$	$298 \leq T \leq 933$	$\Delta_f G^\circ = -2318737.7401 + 435.7241T$	1.0000	[+2.45; −2.14]
	$933 \leq T \leq 1500$	$\Delta_f G^\circ = -2354465.4194 + 473.8687T$	1.0000	[−1.22; +1.61]
		$\Delta_f H^\circ = -2371004.8863 + 14.0389T$	0.9945	[+1.47; −1.77]
		$\Delta_f S^\circ = -487.7358 + 0.0115T$	0.9992	[−2.22; +3.01]
	$1500 \leq T \leq 2100$	$\Delta_f G^\circ = -2343286.1443 + 466.4599T$	1.0000	[−1.77; +2.43]
		$\Delta_f H^\circ = -2385491.1627 + 23.7619T$	0.9988	[+1.34; −1.49]
$\Delta_f S^\circ = -490.2696 + 0.0132T$		1.0000	[−0.84; −1.67]	
$\text{Al}_2\text{OC}$	$1983.05 \leq T \leq 2100$	$\Delta_f G^\circ = -615041.7130 + 123.2766T$	1.0000	[−0.37; +0.41]
		$\Delta_f H^\circ = -682074.8196 + 32.8558T$	1.0000	[+0.14; −0.25]
		$\Delta_f S^\circ = -156.1373 + 0.0161T$	1.0000	[−0.20; +0.21]

Table A.4

Exactness of Ülich approximation (%)

Temperature interval (K)	$\text{Al}_2\text{O}_3$ $\Delta_f H^\circ; \Delta_f S^\circ$	$\text{Al}_4\text{C}_3$ $\Delta_f H^\circ; \Delta_f S^\circ$	$\text{Al}_4\text{O}_4\text{C}$ $\Delta_f H^\circ; \Delta_f S^\circ$	$\text{Al}_2\text{OC}$ $\Delta_f H^\circ; \Delta_f S^\circ$
298–933	+0.0508, −0.1397; +0.6422, −0.9143	+0.6687, −0.4143; +7.3328, −2.2263	+0.0878, −0.1386; +1.1357, −0.8813	
933–1500	+0.1530, −0.2262; +0.7783, −0.8150	−0.4468, +0.2249; −1.1807, +0.4278	+0.1299, −0.2095; +0.6397, −0.7313	
1500–2100	+0.2519, −0.3024; +0.8254, −0.7777	+0.6747, −1.4357; +1.1054, −1.8599	+0.2665, −0.3432; +0.8454, −0.8549	
1983.05–2100				+0.3040, −0.3208; +0.7593, −0.7679

Table A.5

Comparison of discrete Janaf data with a number of equations

Equations	Intervals of relative errors (%)	
(45), (46), (47), (53), (60), (61), (62), (63), (79)	Abs. R.E. $< 5.10^{-2}$	[−1.55; +1.96]; [−1.48; +1.78]; [−2.15; +2.98]; [+4.04; −3.74]; [+1.02; −1.07]; [−1.16; +0.90]; [+3.08; −3.12]; [−4.66; +3.69]; [−3.40; +1.09] <sup>a</sup>
(31), (32), (33), (51), (52), (73), (74), (80)	Abs. R.E. $< 32.1 \times 10^{-2}$	[−4.79; +5.06]; [+7.06; −6.78]; [−8.68; +8.11]; [+8.6; −11.86]; [+4.29; − 5.05]; [−29.74; +32.08]; [−11.07; +12.04]; [−5.40; +8.92] <sup>a</sup>
(29), (72), (78)	Abs. R.E. $< 1.751$	[−1.3940; +1.4339]; [+1.10; −0.90]; [+1.7316; −1.7509]

<sup>a</sup> All limits to be multiplied by  $10^{-2}$ .

## References

- Wang, Z., Liu, X., Zhang, J. and Bian, X., Study of the reaction mechanism in the Al–C binary system through DSC and XRD. *J. Mater. Sci.*, 2004, **39**, 2179–2181.
- Foerster, C. E., Fitz, T., Dekorsky, T., Prokert, T., Kreißig, U., Mücklich, A. et al., *Surf. Coat. Tech.*, 2005, **192**, 317–322.
- Wykes, M., Counsell, G., McGlinchey, D. and Wu, C. H., Tokamak dust, characterization and removal studies. In *Proceedings of the 21st Symposium on Fusion Technology*, 2000.

4. Kiehl, J. P. and Kuster, D., Nouveaux réfractaires à haute teneur en alumine et leur procédé d'obtention. European Patent 0168295 (June 11, 1985).
5. Dubots, D. and Toulouse, P., Multiphase electro-melted material based on alumina + aluminium oxycarbide and oxynitride. Patent WO 89/08624 (September 21, 1989).
6. Khalifa, W., Samuel, F. H. and Gruzleski, J. E., Influence of inclusions on the nucleation of the  $\alpha$ -Al phase in Al–Si–Fe alloys. In *Adv. Mater. Conf.*, 2003.
7. Riley, F. L., Aluminum oxide. In *Advanced Ceramic Materials*, ed. R. J. Brook. Pergamon Press, Oxford, 1991, pp. 10–13.
8. Lihmann, J. M., Zambetakis, T. and Daire, M., High temperature behavior of the aluminum oxycarbide  $Al_2OC$  in the system  $Al_2O_3$ – $Al_4C_3$  and with additions of aluminum nitride. *J. Am. Ceram. Soc.*, 1989, **72**(9), 1704–1709.
9. Kingery, W. D., Bowen, H. K. and Uhlmann, D. R., *Introduction to Ceramics (2nd ed.)*. John Wiley and Sons, New York, 1976.
10. Larrère, Y., Willer, B., Lihmann, J.-M. and Daire, M., Diagrammes d'équilibre stable et métastable dans le système  $Al_2O_3$ – $Al_4C_3$ . *Rev. Int. Hautes Temp. Réfract. Fr.*, 1984, **21**, 3–18.
11. Lihmann, J. -M., Nouvelles céramiques dans le système C–Al–O–N; étude de la résistance à l'usure. D. thesis. Université Louis Pasteur, Strasbourg (Fr), 1982.
12. Lihmann, J. M., Tirlocq, J., Descamps, P. and Cambier, F., Thermodynamics of the Al–C–O system and properties of SiC–AlN– $Al_2OC$  composites. *J. Eur. Ceram. Soc.*, 1999, **19**, 2768–2787.
13. Cox, J. H. and Pidgeon, L. M., An investigation of the aluminium–oxygen–carbon system. *Can. J. Chem.*, 1963, **41**, 671–683.
14. Kubaschewski, O. and Evans, E. L., *Metallurgical Thermochemistry (3rd ed.)*. Pergamon Press, Oxford, 1958 [French transl., Gauthier-Villars éd., Paris, 1964].
15. JANAF, *Thermochemical Tables (2nd ed.)*. National Bureau of Standards, Gaithersburg, MD (USA), 1971.
16. Gaskell, D. R., *Introduction to Metallurgical Thermodynamics (2nd ed.)*. Mc Graw-Hill, New York, 1981.
17. Yokokama, H., Fujishige, M., Ujje, S. and Dokiya, M., Phase relations associated with the aluminium blast furnace: aluminium oxycarbide melts and Al–C–X (X=Fe,Si) liquid alloys. *Metall. Trans. B*, 1987, **18**, 433–444.
18. Argonne Natl. Laboratory Comm., Intern. Nuclear Safety Center, 2005.
19. Lewis, G. N. and Randall, M., In *Thermodynamics*, ed. K. S. Pitzer and L. Brewer. 2nd ed. Rev. Mc Graw Hill, New York, 1961.
20. *Handbook of Chemistry and Physics*, ed. D. R. Lide. 1995–1996, pp. 6–109.